Effect of modeling parameters on DEM simulation of CPT measurements in granular materials

Ali Khosravi
Oregon State University, Corvallis, USA, ali.khosravi@oregonstate.edu

Alejandro Martinez[1], Jason DeJong[2]
University of California Davis, Davis, USA, amart@ucdavis.edu[1], jdejong@ucdavis.edu[2]

ABSTRACT: A 3D Discrete Element Method (DEM) model was used to simulate cone penetration tests (CPT) in a virtual calibration chamber (VCC). The main objective of this study is to evaluate the effect of changes in the modeling parameters that control inter-particle interactions as well as the VCC size, stress conditions applied on the specimen, and sleeve friction coefficient on the simulated tip resistance (q_c) and friction sleeve (f_s) measurements. These results are complemented with particle displacements, rotations, and contact forces to provide insight into the differences in measured CPT response. The results of this study show the important effect of inter-particle contact properties, interface characteristics, and chamber size on the q_c and f_s measurements. In addition, the results of the DEM simulations are also used to further detail current soil behavior type (SBT) charts with the effect of modeling parameters and boundary conditions.

Keywords: cone penetration test, discrete element modeling, site characterization, calibration chamber5

1. Introduction

Accurate stratigraphy characterization and estimation of soil engineering properties, such as shear strength and density, are required for engineering analysis and design of geotechnical structures and systems. Challenges associated with estimation of soil engineering properties include the dependency of soil behavior on state variables, such as state of stresses and density, and the effects of soil fabric or microstructure. Due to the difficulty and high costs involved in obtaining undisturbed samples of coarse-grained soils for laboratory testing, both researchers and practitioners have focused on developing correlations between measurements from in-situ tests, such as the Cone Penetration Test (CPT) and the Dilatometer Test (DMT), and soil properties and state variables.

The CPT has recently received significant attention due to its high repeatability and accuracy, high data resolution, robustness, and industry familiarity. Numerous empirical correlations between CPT measurements, such as the tip resistance (q_c), friction sleeve (f_s), and pore pressure (u_2), and properties such as friction angle, relative density, and unit weight have been developed during the last four decades [e.g. 1-3]. These correlations have been developed based on laboratory calibration chamber tests or on comparison of field measurements with results from laboratory element tests. Calibration chamber tests provide the opportunity of obtaining CPT measurements on well-characterized soil specimens. However, they can be time consuming and expensive due to the large volume of soil required for every sounding. In addition, these tests only provide boundary measurements. Thus, the lack of knowledge of the soil deformation mechanisms, and how they change with soil properties and state, can add uncertainty in the predictions from these correlations.

Analytical and numerical modeling have helped further shed light into the factors and mechanisms that affect CPT measurements. Analytical studies based on bearing capacity, strain path, and cavity expansion [e.g. 4-7], along with numerical studies employing finite difference and finite element techniques [e.g. 8-10] have shed light into the effect of soil properties on CPT measurements. These investigations have employed continuum-based approximations that provide realistic predictions of soil behavior. However, these methods do not explicitly consider inter-particle and probe-particle interactions, which fundamentally control the behavior of coarse-grained soils [11].

Discrete Element Modeling (DEM) simulations provide the ability to investigate the behavior of granular materials in light of particle-level information, such as inter-particle forces and particle kinematics. Using DEM simulations, the deformation behavior of granular materials can be simulated form the interactions between individual particles [12]. Previous numerical studies of CPT penetration using DEM have investigated the role of deformation mechanisms and soil dilatancy along with the effects of boundary conditions, probe diameter to particle size ratio effects, and particle shape and crushing on the CPT measurements and on the stresses and strains developed around the probe [13-19]. These investigations have provided insightful information on the influence of state variables and calibration chamber boundary effects on the penetration resistance. The goal of the investigation presented here, in contrast, is to evaluate the ability of DEM simulations to simulate realistic q_c and f_s measurements. This is done through comparison of q_c and f_s results from simulations performed with varying configuration, assembly properties, and contact parameters, along with interpretation of results using the Soil Behavior Type (SBT) framework commonly used in practice.

2. Discrete Element Model

All the simulations described here were performed using PFC^{3D} from Itasca, Inc. (2014). The CPT soundings were performed inside a cylindrical Virtual Calibration Chamber (VCC) with a height of 1.0 m and a diameter of

0.7 m (Figure 1a). The VCC's top and radial walls imposed constant stress boundary conditions on the specimens contained within them. The specimens were either K_0-consolidated, with a vertical stress, σ'_v, of 100 kPa and a horizontal stress, σ'_h, of 50 kPa, or isotropically consolidated, with σ'_v of 100 kPa. The CPT probe had a diameter of 0.044 m and a tip with an apex angle (2θ) of 60° (Figure 1a). The cone tip was followed by a friction sleeve with a length of 0.16 m. This probe geometry is equivalent to that in CPT probes with a cross-sectional area of 15 cm^2.

The simulated granular material was simulated the behavior of Ottawa 20-30 sand. The grain size distribution of Ottawa 20-30 sand was scaled up by a factor of 20 to reduce the number of particles in the model and decrease computational cost, as shown in Figure 2. This led to a mean particle size of 14.4 mm. The specimens contained in the VCC were composed of about 160,000 spherical particles. The VCC geometry and particle sizes used in this study resulted in a chamber diameter to probe diameter ratio ($D_{chamber}/D_{probe}$) of 15.9 and in a probe diameter to mean particle size ratio (D_{probe}/D_{50}) of 3.1. While these values are smaller than those employed in experimental calibration chamber tests, they are consistent with previous 3D DEM studies which employed $D_{chamber}/D_{probe}$ values between 10.5 and 16.7 and D_{probe}/D_{50} values between 2.7 and 3.3 [15, 17, 19, 20]. In all the simulations the probe was advanced at a rate of 0.05 m/s to a depth of 0.6 m.

The baseline model parameters, shown in Table 1, were calibrated against triaxial compression tests with Ottawa 20-30 sand, as described in [21, 22]. The linear contact model with rolling resistance was employed in this investigation to model the effects of particle angularity on the response of the simulated granular material. Mass scaling was used in this investigation to decrease the computational time. This was done by upscaling the particle density by a factor of 10. Triaxial compression simulations with the baseline parameters indicate a critical state friction angle of 30.9° and a peak friction angle of 44.5° at a confining pressure of 100 kPa. The coefficient of friction between the probe and the particles was selected as 0.2, in agreement with measurements by [23, 24], while the coefficient of friction between the chamber walls and the probe was 0.1. The simulation parameters and configuration described here led to an inertial number, I, of 3.4 x 10^{-3}, obtained following the method outlined by [25]. Since the inertial number was smaller than 10^{-2}, it can be assumed that the simulation conditions were quasi-static throughout the penetration simulation, in accordance with [26].

The specimens were generated using the boundary contraction method. Initially, a cloud of frictionless particles was created, which was allowed to reach equilibrium until the effective stress became close to zero. Afterwards, the testing inter-particle friction and rolling resistance coefficients were set to the testing values, and the servo-control mechanism was activated to consolidate the specimen. This process led to specimens with homogenous void ratio, as shown in Figure 1b.

Table 1. Baseline DEM simulation parameters.

Parameter	Value
Ball-Ball Coefficient of Friction, μ_{BB}	0.40
Rolling Resistance Coefficient, μ_{RR}	0.175
Damping Coefficient	0.05
Ball Density (kg/cm^3)	26500
Stiffness Ratio	2
Normal Stiffness, k_n (MN/m)	350
Probe-ball Coefficient of Friction, μ_{PB}	0.20
Chamber-ball Coefficient of Friction	0.10

3. Results

Series of simulations were performed on a K_0-consolidated specimen to investigate the effect of various parameters on the simulated q_c and f_s measurements. The parameters varied include the void ratio (e = 0.59, 0.64, and 0.67), VCC diameter (D_{CH} = 0.5, 0.7 and 1.0 m),

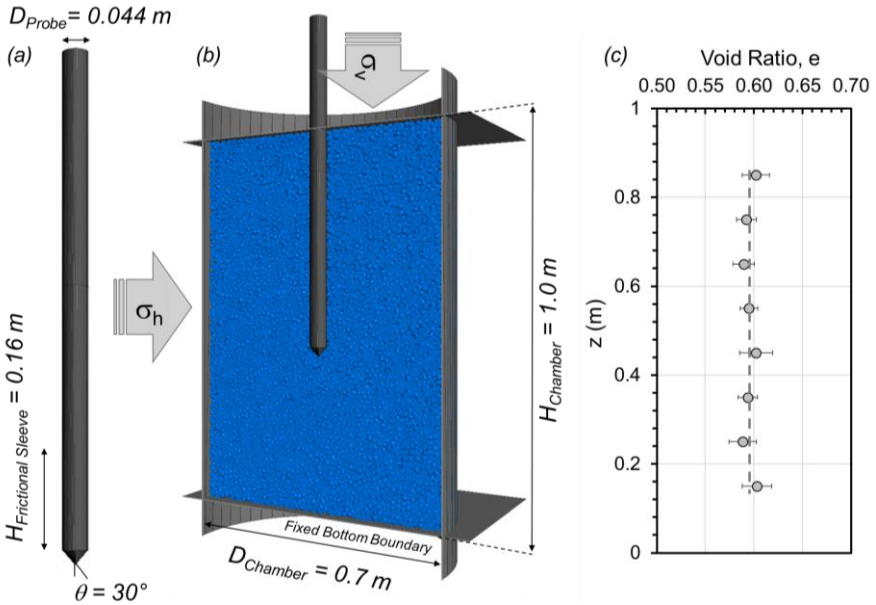

Figure 1. Simulated (a) CPT probe and (b) Virtual Calibration Chamber (VCC), and (c) local void ratio distribution along VCC height (note: error bars show standard deviation in void ratio).

boundary stress conditions ($K = \sigma'_h/\sigma'_v$ = 0.5 and 1.0), inter-particle friction coefficient (μ_{BB} = 0.2, 0.4, and 0.6), the rolling resistance coefficient (μ_{RR} = 0.00, 0.175, and 0.35), and probe-particle friction coefficient (μ_{PB} = 0.2, 0.3, and 0.4). These variations were implemented relative to the baseline parameters, such that only the specified parameter is different to those presented in Table 1.

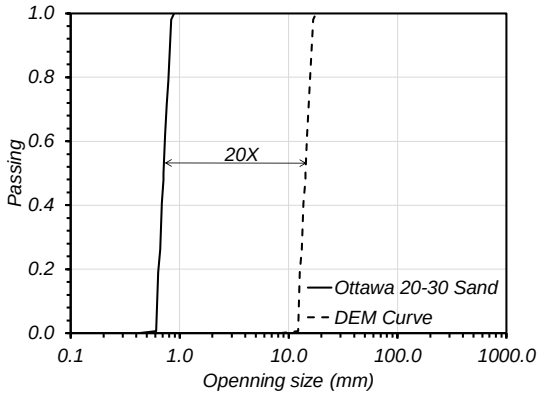

Figure 2. Simulated grain size distribution.

3.1. Baseline Simulation

Tip resistance and friction sleeve measurements from the baseline simulation, with the parameters presented in Table 1, are shown in Figures 3a and 3b. The q_c and f_s measurements indicate a uniform distribution with depth due to the uniform constant stress applied to the specimen (σ'_v = 100 kPa, σ'_h, = 50 kPa).

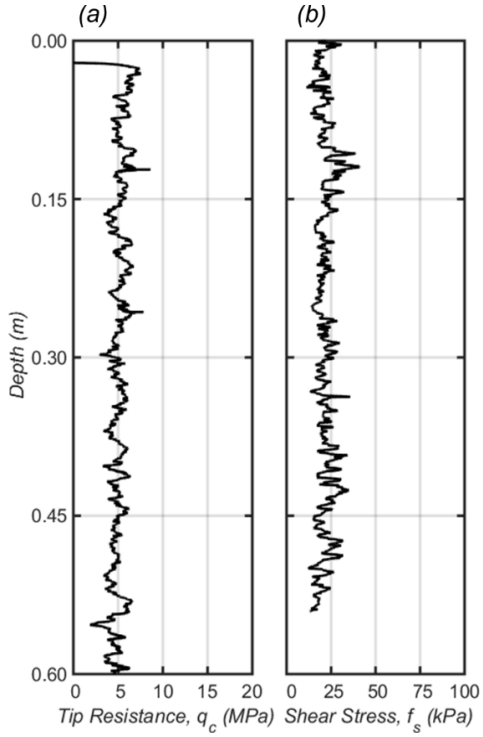

Figure 3. Profiles of (a) q_c and (b) f_s for baseline simulation.

The mean q_c and f_s values for the baseline simulation are 4.8 MPa and 21.6 kPa. These results were plotted on the SBT charts proposed by [27, 28], as shown in Figures 4a and 4b. The classification results indicate an SBT corresponding to "silty sand to sandy silt" according to the Robertson (1990) chart, and slightly "sand-like – contractive) according to the Robertson (2016) chart. Figures 4a and 4b also show representative data points from [28]. The classification of the simulated results is consistent with data points 2, 3, 4, 5, and 7, which are from field soundings in normally consolidated sands and sandy tailings. These results highlight the ability of the DEM model and the calibration parameters to successfully capture the behavior of coarse-grained soils and reproduce realistic CPT measurements.

An initial step in this investigation was to assess the variability of the q_c and f_s measurements. To do so, three simulations were performed with the same modeling parameters and testing conditions but on three different specimens. Differences in the results can result from differences in packing and potential heterogeneities in the specimens. These simulations indicate a relatively small amount of variability, with differences of up to 6.5% and 5.7% for the q_c and f_s measurements, respectively.

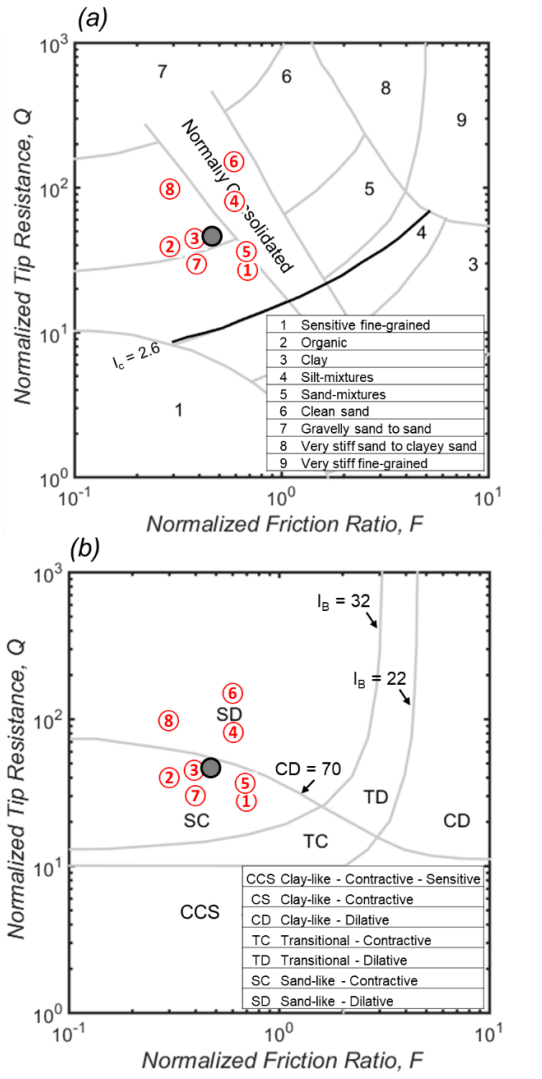

Figure 4. Results from baseline simulation plotted on (a) Robertson (1990) and (b) Robertson (2016) CPT-based soil classification charts.

3.2. Parametric Study

The void ratio of a coarse-grained soil specimen or deposit has been shown to have an important effect on the

tip resistance and friction sleeve measurements. In general, denser soils lead to larger q_c and f_s measurements due to their greater shear strength and to the greater increase in mean effective stresses developed around the CPT probe during penetration [e.g. 29]. Simulations were performed on specimens with initial void ratios of 0.59, 0.64, and 0.67. The measurements increased significantly as the void ratio was decreased, as shown in Figure 5a, with q_c and f_s values of 4.8 MPa and 21.6 kPa for the denser specimen and of 3.5 MPa and 15.1 kPa for the looser specimen.

These simulation results can be used to evaluate whether the results agree with predictions from empirical correlations between q_c and relative density. For this exercise, the procedure outlined by [30] was adopted. To complete this comparison, maximum and minimum void ratio values equal to those for Ottawa 20-30 sand were assumed (e_{max} = 0.72, e_{min} = 0.48) to obtain void ratio values predicted from the simulated q_c measurements. The void ratios predicted by the correlation are of 0.65, 0.66, and 0.68, indicating that the void ratio of the denser specimen was overpredicted while the void ratio of the looser specimen was more closely predicted. This comparison indicates similarities in the trends from numerical and experimental tests; however, it also highlights that quantitative differences that may be due to factors such as the lack of particle crushing in the simulations, the assumed values for the extreme void ratios, or differences in behavior between the simulated granular material and the sands used to develop the empirical correlation.

Significant efforts have been devoted to understanding the effects of the boundary conditions imposed by calibration chambers on the q_c and f_s measurements. This work has led to correction factors to account for boundary condition effects. In this manner, calibration chamber results can approximate those obtained from field tests [e.g. 2, 3, 31]. Simulations on specimens confined under different stress conditions indicate an important influence of the lateral earth pressures coefficient, K, on the magnitude of q_c and f_s measurements. As shown in Figure 5b, the q_c and f_s magnitudes sharply increase, from values of 4.8 MPa and 21.6 kPa to values of 12.1 MPa and 63.7 kPa as the K coefficient is increased from 0.5 to 1.0. These results agree with the fact that soil shear strength increases with effective stress.

Previous work has also shown that the results from CPT simulations are influenced by the VCC diameter [e.g. 17]. To further investigate the potential effects, simulations were performed on specimens contained within chambers with diameters of 0.5, 0.7 and 1.0 m, which were composed of 82,000, 160,000 and 330,000 particles, respectively. The results indicate that the q_c and f_s magnitudes systematically increase as the chamber diameter is increased (Figure 5c). These results are in general agreement with results from [32] indicating that chambers with smaller diameters with stress-controlled boundary stresses lead to smaller values of tip resistance. Insertion of a probe in a calibration chamber requires for an additional volume equal to that of the advancing probe to be accommodated by soil densification and retraction of the chamber's boundaries. This retraction of the boundaries results in a relaxation of the cavity pressure and consequently a decrease in tip resistance. This trend is evident in the measurements of particle displacements presented in Figures 6a through 6c. As shown, particles within a larger zone around the probe displace in simulations in smaller chambers. This results in a decrease of the normal stress acting against the probe. In fact, the normal stress acting against the friction sleeve decreased from 151.6 kPa to 76.7 kPa as the chamber diameter was decreased from 1.0 to 0.5 m.

The strength and deformation behavior of granular material depends on intrinsic soil properties such as particle shape, size, surface roughness, and mineralogy, along with other parameters such as gradation [e.g. 33]. DEM offers the ability of systematically varying modeling parameters which approximate the influence of these intrinsic properties. For instance, particle shape can be either explicitly simulated with non-spherical particles

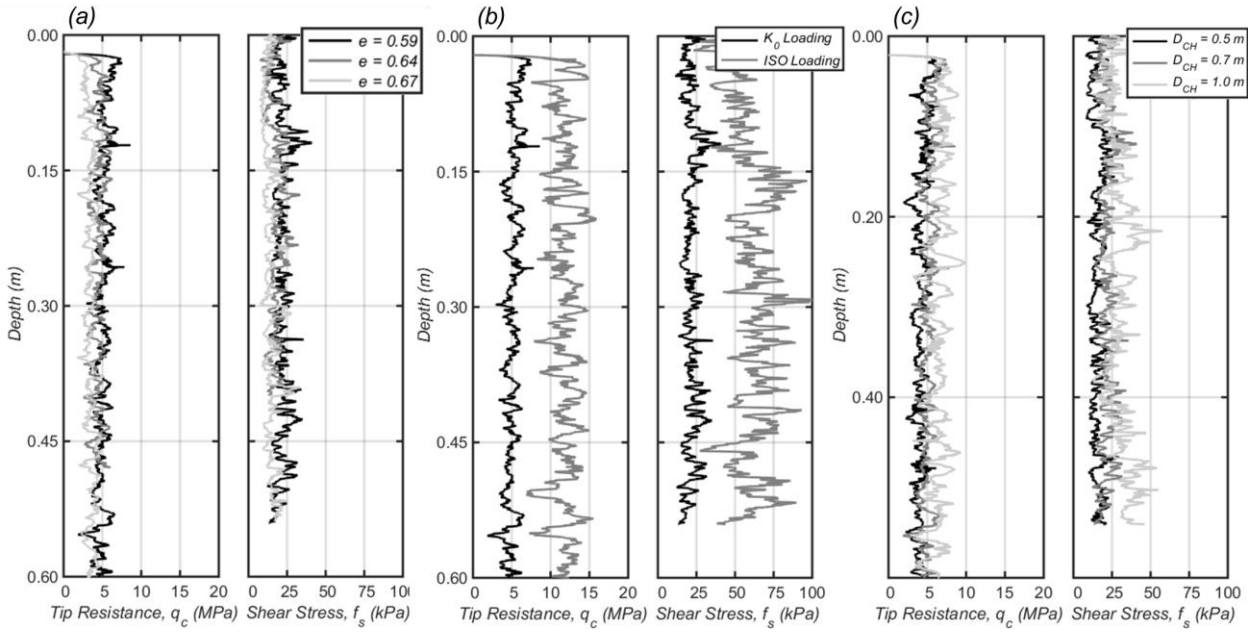

Figure 5. Profiles of (a) q_c and (b) f_s for simulations with varying (a) void ratio, e, (b) stress boundary conditions, and (c) chamber diameter, D_{CH}.

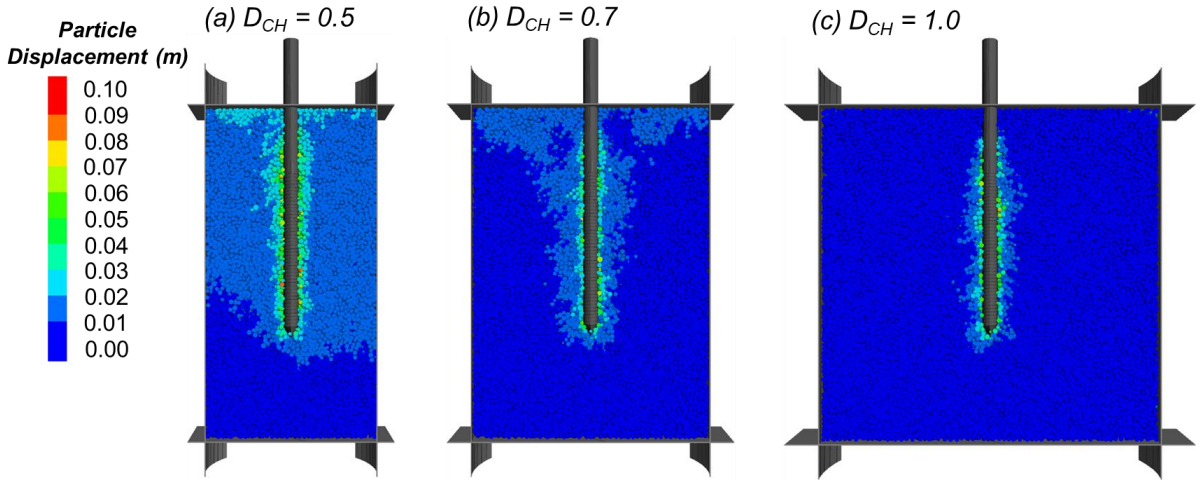

Figure 6. Particle displacements along vertical cross sections for simulations on VCCs of different diameter Note: all measurements taken at a CPT penetration depth of 60 cm.

[e.g. 34-37], or it can be approximated using a rolling resistance coefficient [e.g. 38-40], as done in this study. Similarly, the effects of particle surface roughness and mineralogy can be simulated by the inter-particle friction coefficient, while other parameters such as contact stiffness can also approximate the influence of mineralogy. Finally, specialized contact models that consider particle crushing can be implemented, as described in [19, 41]

In this study, the values of the μ_{BB}, μ_{RR}, and μ_{PB} coefficients were varied to approximate the effects of changes in particle morphology and CPT friction sleeve surface roughness. The simulations indicate that the simulated q_c and f_s magnitudes increase as the μ_{BB} is increased, as shown in Figure 7a. An initial increase in μ_{BB} from 0.2 to 0.4 led to a steep increase of 59% in q_c while a further increase in μ_{BB} from 0.4 to 0.6 resulted in a more modest increase of 15%. These results are in general agreement with trends reported by [42, 443] reflecting the transition from particle motions that are dominated by sliding at low μ_{BB} values to motions that are dominated by rolling at higher μ_{BB} values. The magnitude of the inter-particle friction coefficient resulted in smaller changes on the f_s measurements, which increased by 15% and 20% as a result of μ_{BB} increases of 0.2 to 0.4 and 0.4 to 0.6, respectively. This trend is in agreement with results from [23, 44, 45] indicating that the strength of soil-structure interfaces depends both on the internal strength of the soil as well as on the surface roughness of the solid material.

The inter-particle friction coefficient also has an influence on the interactions between the CPT probe and the particles. Figures 8a to 8c show force chain maps of simulations with varying μ_{BB}, where contact forces larger than 150 N and smaller than 20 N are shown and the thickness of the lines is proportional to their magnitude. As shown, larger μ_{BB} values result in force chains that propagate to a larger zone around the probe tip, indicating that more stable force chains are developed with these modeling parameters.

Changes in the rolling resistance coefficient resulted in similar but stronger effects on the simulated q_c and f_s

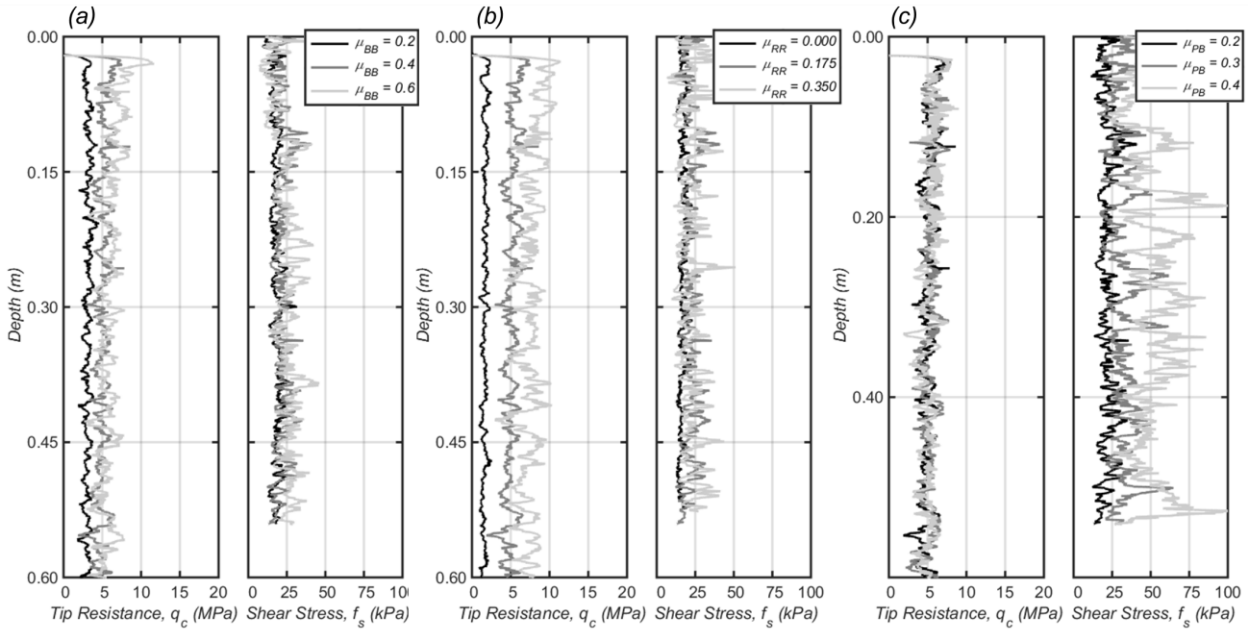

Figure 7. Profiles of (a) q_c and (b) f_s for simulations with varying (a) interparticle friction ratio, μ_{BB}, (b) rolling resistance coefficient, μ_{RR}, and (c) probe-particle friction coefficient, μ_{PB}.

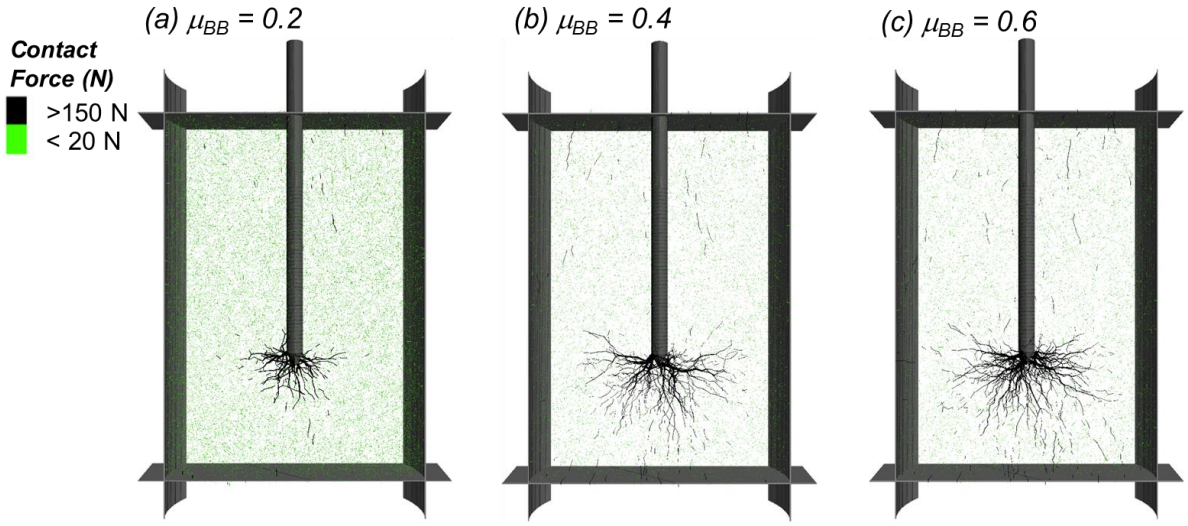

Figure 8. Force chain maps along vertical cross section for simulations with inter-particle friction coefficients of (a) 0.2, (b) 0.4, and (c) 0.6. Note: all measurements taken at a CPT penetration depth of 60 cm.

measurements as the changes in the inter-particle friction coefficient, as shown in Figure 7b. Namely, the q_c values increased by 213% and 57% as the μ_{RR} was increased from 0 to 0.175 and from 0.175 to 0.35, respectively. Also, the f_s values increased more modestly, by 33% and 6% for the same increases in μ_{RR}. Inspection of the force chain maps suggests similar effects on the probe-particles interactions, where larger μ_{RR} values lead to larger contact forces that are located within a zone of greater size around the probe's tip.

The effect of the friction sleeve surface roughness on the f_s measurements, which has been subject to a significant amount of research [e.g. 46-48], can be modeled in DEM with changes in the probe-particle friction coefficient. As shown in Figure 7c, these simulations were performed with μ_{PB} values of 0.2, 0.3, and 0.4, which resulted in f_s measurements of 21.6, 34.0 and 53.0 kPa, respectively. These measurements are consistent with DEM and experimental results from [23, 24]. Interestingly, the changes in μ_{PB} had a negligible effect on the tip

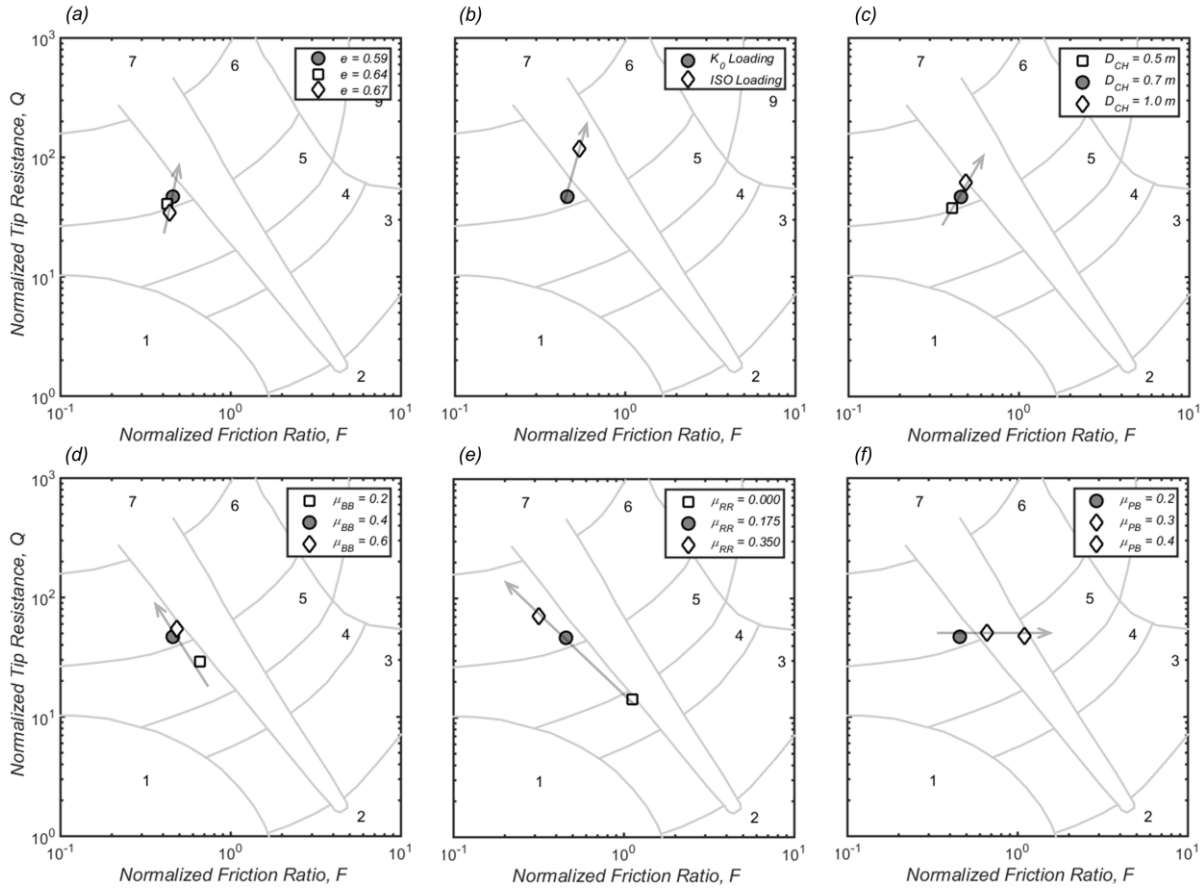

Figure 9. Normalized CPT soil behavior type classification of simulations with varying (a) void raito, (b) boundary conditions, (c) chamber diameter, (d) inter-particle friction coefficient, (e) rolling resistance coefficient and (f) varying probe-particle friction coefficient.

resistance measurements, with differences of less than 10% between the simulations.

4. Soil Behavior Type (SBT) Classification

Soil behavior type classification offers the ability of estimating the expected behavior of a given soil and efficiently assessing the stratigraphy of a site. SBT reflects the mechanical response of soil to the loading imposed by the CPT probe during penetration. Thus, while the SBT classification may not directly match a classification based on index properties, it reflects the characteristic behaviors of different soil types, such as strength, stiffness, density, overconsolidation ratio (OCR), aging, and sensitivity [28].

The q_c and f_s measurements from the DEM simulations were used to determine normalized tip resistance, Q, and friction ratio, F, parameters, which were plotted in Robertson's (1990) soil classification chart (Figures 9a through 9f). The data points move in the soil classification chart in the following manner: (i) up as the void ratio is decreased, (ii) up and to the right as the K parameter is increased, (iii) up and to the right as the chamber diameter is increased, (iv) up and to the left as the inter-particle friction coefficient is increased, (v) up and to the left as the rolling resistance coefficient is increased, and (vi) directly right as the probe-particle friction coefficient is increased. Figure 10a shows the trends reported in Robertson (1990), while Figures 10b and 10c show the trends from DEM simulations in Robertson's (1990) and Robertson's (2016) space. This comparison indicates similar trends in experimental and numerical results. Namely, the data points move up as parameters that affect soil's the shear strength and density are increased, such as the friction angle and the relative density for experimental results and the inter-particle friction coefficient and rolling resistance coefficient and void ratio for the DEM simulations. Field trends indicate that increases in OCR, which is related to the lateral earth pressures coefficient, result in an upward and rightward movement of the datapoints, which agrees with the trends from numerical results.

The numerical results can also be used to investigate shifts in the data resulting from the testing conditions. For instance, the DEM simulations showed a measurable influence of the calibration chamber diameter on both the q_c and f_s measurements as well as on the SBT classification (Figures 5c and 9c). Also, increases in the probe-particle friction coefficient showed a steep increase in f_s and shift in SBT classification (Figures 7c and 9f). DEM simulations provide the ability of performing tests and measurements that can be challenging to achieve experimentally (e.g. careful changes in void ratio or changes in particle morphology). Thus, once successfully calibrated, this type of investigations can complement experimental investigations on, for example, determining correction factors for calibration chamber tests, investigating changes in localized penetration failure mechanisms, and determining the effect of individual index properties on SBT classification.

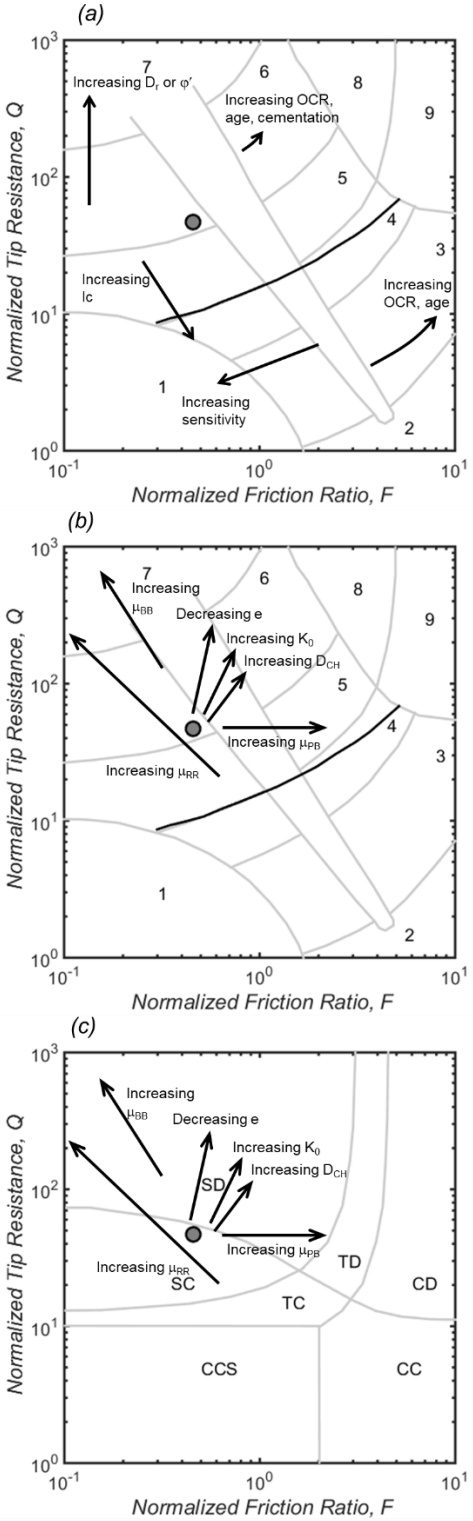

Figure 10. SBT trends reported by Robertson (1990) and trends from DEM simulations on (a) Robertson's 1990 and (b) Robertson's 2016 chart for soil behavior type classification.

5. Conclusions

This paper provides the results of a numerical parametric study that evaluates the ability of 3D DEM to simulate realistic CPT q_c and f_s measurements. The simulations were performed on specimens contained within a virtual calibration chamber (VCC), where the changes in q_c and f_s measurements as a result of specimen void ratio, stress boundary conditions, VCC diameter, and inter-par-

ticle friction, rolling resistance, and probe-particle friction coefficients were investigated. The baseline simulation yielded realistic q_c and f_s measurements of 4.8 MPa and 21.6 kPa, respectively. In general terms, changes in parameters that increase the shear strength of the simulated granular material resulted in increases in q_c and f_s, in agreement with trends from experimental tests. In addition, the simulations provide insight into artificial effects of the VCC size and the probe's surface properties. Interpretation of the results using the Soil Behavior Type (SBT) framework also indicates that the numerical trends are in agreement with field experiments. DEM numerical investigations provide the opportunity to perform tests on conditions that may be challenging to achieve experimentally. Such studies can be used to complement experimental investigations and to further the understanding of aspects such as the influence of soil intrinsic properties on CPT measurements, penetration failure mechanisms and SBT classification, and the effects of the calibration chamber boundary and the CPT probe conditions.

Acknowledgement

This material is based upon work supported in part by the National Science Foundation (NSF) under NSF CA No. EEC-1449501. Any opinions, findings and conclusions or recommendations expressed in this material are those of the author(s) and do not necessarily reflect those of the NSF.

References

[1] Schmertmann, J. H. "Guidelines for Cone Penetration Test. (Performance and Design)", FHWA Report No. TS-78-209, Federal Highway Administration, Washington, DC: 145 p, 1978.

[2] Baldi G., Bellotti R., Ghionna V. N., Jamiolkowski M., and Pasqualini E. "Interpretation of CPTs and CPTUs, 2nd Part: Drained Penetration of Sands", In: Field Instrumentation and In-situ Measurements, Proceedings of the 4th International Geotechnical Seminar, Singapore, Nanyang Technological Institute, 1986, pp. 143-156.

[3] Jamiolkowski, M., LoPresti D., and Manassero. M. "Evaluation of Relative Density and Shear Strength of Sands from Cone Penetration Test and Flat Dilatometer Test", In: Soil Behavior and Soft Ground Construction (GSP 119), ASCE, Reston/VA, 201-238.

[4] Durgunoglu H. T. and Mitchell J. K. "Static penetration resistance of soils, I-Analysis, II-Evaluation of the Theory and Implications for Practice", In: ASCE Spec. Conference, In situ measurements of soil properties, Raleigh, NC, 1975.

[5] Teh, C.I. and Houlsby, G.T. "An Analytical Study of the Cone Penetration Test in Clay" Géotechnique, 41(1): pp. 17-34, 1991. https://doi.org/10.1680/geot.1991.41.1.17.

[6] Vesic A.S. "Expansion of Cavities in Infinite Soil Mass" Journal of Soil Mechanics Foundation Division, ASCE, 98(SM3), pp. 265-290, 1972.

[7] Salgado, R., Mitchell, J.K., and Jamiolkowski, M. "Cavity eExpansion and Penetration Resistance in Sand", Journal of Geotechnical and Geoenvironmental Engineering, 123(4), pp. 344-354, 1997. https://doi.org/10.1061/(ASCE)1090-0241(1997)123:4(344)

[8] Ahmadi, M. M., and Robertson, P. K. ""Thin Layer Effects on the CPT q_c Measurement", Canadian Geotechnical Journal. 42(9), pp. 1302–1317, 2005. https://doi.org/10.1139/t05-036

[9] Yu, H. S., Herrmann, L. R., and Boulanger, R. W. "Analysis of Steady Cone Penetration in clay", Journal of Geotechnical and Geoenvironmental Engineering, 126 (7), pp. 594–605, 2000. https://doi.org/10.1061/(ASCE)1090-0241(2000)126:7(594)

[10] Susila, E. and R. D. Hryciw. "Large displacement FEM Modeling of the Cone Penetration Test (CPT) in Normally Consolidated Soil", International Journal of Numerical and Analytical Methods in Geomechanics, 27(7), pp. 585-602, 2003. https://doi.org/10.1002/nag.287

[11] Mitchell, J.K. and Soga, K. "Fundamentals of Soil Behavior. " Wiley, New York, 558 p, 2005.

[12] Cundall, P. A. and Strack, O. D. L. "A Discrete Numerical Model for Granular Assemblies", Geotechnique, 29(1), pp. 47-65, 1979. https://doi.org/10.1680/geot.1979.29.1.47

[13] Huang, A. B. and Ma, M. Y. "An Analytical Study of Cone Penetration Tests in Granular Material" Canadian Geotechnical Journal, 31(1), pp. 91–103, 1994. https://doi.org/10.1139/t94-010

[14] Jiang, M. J., Yu, H. S., and Harris, D. "Discrete Element Modelling of Deep Penetration in Granular Soils", International Journal for Numerical and Analytical Methods in Geomechanics, 30 (4), pp. 335–361, 2006. https://doi.org/10.1002/nag.473

[15] Arroyo M, Butlanska J, Gens A, Calvetti F, Jamiolkowski M. " Cone Penetration Tests in a Virtual Calibration Chamber", Géotechnique 2011;61(6), pp. 525-31, 2011. https://doi.org/10.1680/geot.9.P.067

[16] McDowell, G. R., Falagush, O., and Yu, H. S. "A Particle Refinement Method for Simulating DEM of Cone Penetration Testing in Granular Materials." Géotechnique Letters, 2(3), pp. 141–147, 2012. https://doi.org/10.1680/geolett.12.00036

[17] Butlanska, J., Arroyo, M., Gens, A., and O'Sullivan, C. "Multi-scale Analysis of Cone Penetration Test (CPT) in a Virtual Calibration Chamber" Canadian Geotechnical Journal, 51(1), 51-66. https://doi.org/10.1139/cgj-2012-0476

[18] Falagush, O. "Discrete Element Modelling of Cone Penetration Testing in Granular Materials", PhD Thesis, University of Nottingham, 2014.

[19] Ciantia, M. O., Arroyo, M., Butlanska, J., and Gens, A. "DEM Modelling of Cone Penetration Tests in a Double-porosity Crushable Granular Material", Computers and Geotechnics, 73, pp. 109-127, 2016. https://doi.org/10.1016/j.compgeo.2015.12.001

[20] Zhang, N., Arroyo, M., Cianta, M.O., Gens, A., and Butlanska, J. "Standard Penetration Testing in a Virtual Calibration Chamber", Computers and Geotechnics. 111(July), pp. 277-289, 2019. https://doi.org/10.1016/j.compgeo.2019.03.021

[21] Su, J., Frost, J.D., and Martinez, A. "Three-dimensional Numerical Assessment of Axial and Torsional Interface Shear Behaviour", In: Proceedings of in 7th International Symposium on Deformation Characteristics of Geomaterials, Glasgow, UK, 2019. https://doi.org/10.1051/e3sconf/20199213016

[22] Su, J. "Advancing Multi-scale Modeling of Penetrometer Insertion in Granular Materials", Ph.D. Dissertation, Georgia Institute of Technology, 2019.

[23] Martinez, A. and Frost, J. D. "The Influence of Surface Roughness Form on the Strength of Sand-Structure Interfaces", Géotechnique Letters, 7(1), pp. 104-111, 2017a. https://doi.org/10.1680/jgele.16.00169

[24] Martinez, A. and Frost, J. D. "Particle-Scale Effects on Global Axial and Torsional Interface Shear Behavior", International Journal of Numerical and Analytical Methods in Geomechanics, 41(3), pp. 400-421, 2017b. https://doi.org/10.1002/nag.2564

[25] Ciantia M.O., O'Sullivan C. and Jardine R.J. "Pile Penetration in Crushable Soils: Insights from Micromechanical Modelling" In: Proceedings of XVII ECSMGE-2019 Geotechnical Engineering Foundation of the Future, Reykjavík, Iceland, 2019, pp-298-317.

[26] Janda, A., Ooi, J. "DEM Modeling of Cone Penetration and Unconfined Compression in Cohesive Solids", Powder Technology, 293(May), pp. 60–68, 2016. https://doi.org/10.1016/j.powtec.2015.05.034

[27] Robertson, P. K. "Soil Classification using the Cone Penetration Test", Canadian Geotechnical Journal, 27(1), pp. 151–158, 1990. https://doi.org/10.1139/t90-014

[28] Robertson, P. K. "Cone Penetration Test (CPT)-based Soil Behaviour Type (SBT) Classification System – an Update", 53(12), pp. 1910-1927, 2016. https://doi.org/10.1139/cgj-2016-0044

[29] Lunne, T. Robertson, P. K., and Powell, J. J. M. "Cone Penetration Testing in Geotechnical Practice", Spon Press, London, 312 p, 1997.

[30] Idriss, I. M., and Boulanger, R. W. "Soil Liquefaction during Earthquakes", Monograph MNO-12, Earthquake Engineering Research Institute, Berkeley, CA, 2008.

[31] Mayne P. W., and Kulhawy F. H. "Calibration Chamber Database and Boundary Effects Correction for CPT Data", In: Proceedings of the 1st International Symposium on Calibration Chamber Testing, ISOCCT 1, Potsdam, New York, 1991, pp. 257-264.

[32] Salgado, R., Mitchell, J. K., and Jamiolkowski, M. "Calibration Chamber Size Effects on Penetration Resistance in Sand", Journal

of Geotechnical and Geoenvironmental Engineering, 124(9), pp. 878–888, 1998. https://doi.org/10.1061/(ASCE)1090-0241(1998)124:9(878)

[33] Santamarina, J. C. "Soil Behavior at the Microscale: Particle Forces", In: Proceedings of the Symposium on Soil Behavior and Soft Ground Construction, in Honor of Charles C. Ladd - October. MIT, 2001.

[34] Ashmawy, A. K., Sukumaran, B., and Hoang, V. V. "Evaluating the Influence of Particle Shape on Liquefaction Behavior using Discrete Element Simulation", In: Prov. 13th Int. Offsh. Pol. Eng. Conf., Honolulu, HI. 2003, pp. 542-549.

[35] Alonso-Marroquin, F., Luding, S., Herrmann, H. J., and Vardoulakis, I. "Role of Anisotropy in the Elastoplastic Response of a Polygonal Packing", Phys. Rev. E 71, 051304, 2005. 10.1103/PhysRevE.71.051304

[36] Zhou, B, Huang, R. Q., Wang, H. B., Wang, J. F. "DEM Investigation of Particle Anti-rotation Effects on the Micromechanical Response of Granular Materials", Granular Matter, 15(3), pp. 315–26, 2013. https://doi.org/10.1007/s10035-013-0409-9

[37] Kawamoto, R., Ando, E., Viggiani, G., and Andrade J. E. "Level Set Discrete Element Method for Three-dimensional Computations with Triaxial Case Study" Journal of the Mechanics and Physics of Solids, 91, pp. 1 – 13, 2016. https://doi.org/10.1016/j.jmps.2016.02.021

[38] Bardet, J. P. "Observations on the Effect of Particle Rotations on the Failure of Idealized Granular Materials", Mechanics of Materials, 18(2), pp. 159-182, 1994. https://doi.org/10.1016/0167-6636(94)00006-9

[39] Iwashita, K., and Oda, M." Rolling Resistance at Contacts in Simulation of Shear Band Development by DEM", Journal of Engineering Mechanics, 124(3), pp. 285-292, 1998. https://doi.org/10.1061/(ASCE)0733-9399(1998)124:3(285)

[40] Jiang, M., Leroueil, S., Zhu, H., Yu, H. S., and Konrad, J. M. "Two-dimensional Discrete Element Theory for Rough Particles" International Journal of Geomechanics, 9(1), pp. 20-33, 2009. https://doi.org/10.1061/(ASCE)1532-3641(2009)9:1(20)

[41] Chen, Y. P., Bolton, M. D., and Nakata, Y. "Crushing and Plastic Deformation of Soils Simulated using DEM", Geotechnique, 54(2), pp. 131-141, 2004. https://doi.org/10.1680/geot.2004.54.2.131

[42] Thornton, C. "Numerical Simulations of Deviatoric Shear Deformation of Granular Media", Géotechnique, 50(1), pp. 43-53, 2000. https://doi.org/10.1680/geot.2000.50.1.43

[43] Kruyt, N. P. and Rothenburg, L. "Shear Strength, Dilatancy, Energy and Dissipation in Quasi-static Deformation of Granular Materials", Journal of Statistical Mechanics: Theory and Experiment. 7, pp. 1–13, 2006. 10.1088/1742-5468/2006/07/P07021

[44] Uesugi, M. and Kishida, H., "Frictional Resistance at Yield Between Dry Sand and Mild Steel" Soils and Foundations, 26(4), pp. 139-149, 1986. https://doi.org/10.3208/sandf1972.26.4_139

[45] Hebeler, G. L., Martinez, A. and Frost, J. D. "Shear Zone Evolution of Granular Soils in Contact with Conventional and Textured CPT Sleeves", KSCE Civ. Eng. J., 20(4), pp. 1267-1282, 2016. https://doi.org/10.1007/s12205-015-0767-6

[46] Zuidberg, H. M., Schaap, L. H. J., and Beringen, F. L. "A Penetrometer for Simultaneous Measurement of Cone Resistance, Sleeve Friction, and Dynamic Pore Pressure", In: Proceedings of the 2nd European Symposium on Penetration Testing, ESOPT-II, Amsterdam, 2, 1982, pp. 963-970.

[47] Jekel, J. W. A. " Wear of the Friction Sleeve and Its Effect on the Measured Local Friction", In: Proceedings of the International Symposium on Penetration Testing, ISOPT-1, Orlando, 2, 1988, pp. 805–808.

[48] DeJong, J.T., and Frost, J.D. "A Multi-sleeve Friction Attachment for the Cone Penetrometer", Geotechnical Testing Journal, 25(2), pp. 111–127, 2002. doi:10.1520/GTJ11355J.